Photon Signals from Quarkyonic Matter

Giorgio Torrieri,[1,2,*] Sascha Vogel,[1,3,†] and Bjørn Bäuchle[1,‡]

[1]FIAS, Goethe Universität, Ruth-Moufang-Strasse 1, 60438 Frankfurt am Main, Germany
[2]Pupin Physics Laboratory, Columbia University, 538 West 120th Street, New York, New York 10027, USA
[3]SUBATECH, Laboratoire de Physique Subatomique et des Technologies Associées, University of Nantes, IN2P3/CNRS, Ecole des Mines de Nantes, 4 Rue Alfred Kastler, F-44072 Nantes Cedex 03, France

(Received 6 February 2013; revised manuscript received 8 May 2013; published 3 July 2013)

We calculate the bremsstrahlung photon spectrum emitted from dynamically evolving "quarkyonic" matter and compare this spectrum with that of a high chemical potential quark-gluon plasma as well as to a hadron gas. We find that the transverse momentum distribution and the harmonic coefficient is markedly different in the three cases. The transverse momentum distribution of quarkyonic matter can be fit with an exponential but is markedly steeper than the distribution expected for the quark-gluon plasma or a hadron gas, even at the lower temperatures expected in the critical point region. The quarkyonic elliptic flow coefficient fluctuates randomly from event to event and within the same event at different transverse momenta. The latter effect, which can be explained by the shape of quark wave functions within quarkyonic matter, might be considered as a quarkyonic matter signature, provided that the initial temperature is low enough that the quarkyonic regime dominates over deconfinement effects and the reaction-plane flow can be separated from the fluctuating component.

DOI: 10.1103/PhysRevLett.111.012301 PACS numbers: 25.75.−q, 25.75.Dw, 25.75.Nq

The study of nuclear matter at moderate ($T \sim$ 0–180 MeV) temperature and large baryochemical potential ($\mu_Q = \mu_B/3 \sim \Lambda_{\mathrm{QCD}} = 250$ MeV) has recently enjoyed new vigorous theoretical [1] and experimental interest.

From the experimental side, this is due to the start of programs specifically aimed at exploring lower energy collisions with the latest detector technology [2–5]. This regime presents both potential for very interesting physics and unique challenges, since an unambiguous lattice exploration is lacking [6–8], effective field theory [9] gives ambiguous predictions, and the system remains profoundly nonperturbative [10,11].

This ambiguity leaves room for qualitatively new phenomena and even new phases of matter to arise. A recent proposal of this kind is "quarkyonic" matter [12–19]. It is motivated by the ambiguity of defining confinement in a system where baryon density ρ_B is high enough that there is $\sim O(1)$ baryon per baryonic volume.

The possibility of quarkyonic matter [12] comes from the asymmetry between the confinement scale in temperature and chemical potential: The amplitude of a gluon loop at finite temperature is $\sim N_c^2$, while a quark-hole loop at finite chemical potential μ_q has amplitude $\sim N_f N_c \mu_q^2$ [12]. While at high temperature ($T \geq \Lambda_{\mathrm{QCD}} \sim N_c^0$) confinement is broken by gluon loops alone, because of asymptotic freedom, at low temperature quark-hole loops need to overpower gluon loops. This requires $\mu_q \sim \sqrt{N_f/N_c}\Lambda_{\mathrm{QCD}}$ at one loop and an even higher exponent z ($1/2 < z < 1$) at more than one loop [20]. As the number of colors might be considered "large," this introduces an extra scale $\sqrt{N_c}\Lambda_{\mathrm{QCD}}$ in momentum space relevant for deconfinement at finite chemical potential. In configuration space, however, the only relevant scale is the interparticle distance, which for one baryon per baryonic volume $\mu_q \sim \Lambda_{\mathrm{QCD}}$ is always $\sim N_c^{-1/3} \to 0$.

Dense matter at $\Lambda_{\mathrm{QCD}} < \mu_Q < \sqrt{N_c/N_f}\Lambda_{\mathrm{QCD}}$, with features of asymptotic freedom in configuration space but features of confinement in momentum space, at $\Lambda_{\mathrm{QCD}} < \mu_q < \sqrt{N_c/N_f}\Lambda_{\mathrm{QCD}}$ is known as quarkyonic matter. This is an interesting idea, but how much of quarkyonic dynamics survives at $N_c = 3$ and $N_f = 2$, 3 is an open question. It has long been known [21–25] that there are significant *qualitative* differences between the $N_c \to \infty$ limit and $N_c = 3$. As argued in Refs. [20,23,24,26], this indicates that the large N_c limit is separated from the real world by a percolation-type phase transition. The quarkyonic matter transition line is therefore bound to be curved in N_c as well as T, μ_B space, the former being accessible only on the lattice.

The existence of quarkyonic matter, having the properties described in Ref. [12], is therefore a matter for experimental investigation, necessitating a quarkyonic matter phenomenology. We shall attempt to develop one in this work, based on the characteristics in Ref. [12] and their consequences explored in Sections 4 and 5 of Ref. [20]. Quark degrees of freedom make an appearance, and their interactions are governed by the Feynman rules of perturbative QCD (pQCD). The equation of state at equilibrium, therefore, is similar to that of an asymptotically free gas of quarks with a Fermi surface at $\mu_q \sim (1-3)\Lambda_{\mathrm{QCD}}$ and low temperature. Unlike "real" pQCD,

however, confinement is still there: Baryons continue to exist, and quark wave functions are localized around baryons. As in the large N_c limit, baryons are also approximately classical objects, well localized in position; they are also dense enough that there is, on average, one baryon per baryonic volume $O(\Lambda_{\rm QCD}^{-3})$ or more. Hence, quark wave functions are *not* the asymptotically free quark wave functions of pQCD but are instead eigenfunctions of a series of potential wells at the location of the baryons [20] (Fig. 2). This is very similar to the dynamics of a free gas of electrons in a metal, where atoms are classical potential wells (as baryons are at large N_c QCD) and electrons are fermions weakly interacting with each other but with wave functions determined by classical potentials (as quarks are supposed to be in quarkyonic matter). Summarizing, any dynamics inside quarkyonic matter will have pQCD interaction vertices, but incoming quark lines will pick up a form factor, reflecting their confinement. Unlike in the vacuum, this form factor will not be "localized" (since percolation is naturally interpreted as the delocalization of quarks [20]), but will reflect the dynamics of *all* baryons of the system [20]. At a single time step in configuration space, the quark wave function looks like (arrows indicate a three-vector, greek indices a four-vector)

$$\Psi(x) \propto \sum_i^{\rm hadrons} \phi(\vec{x} - \vec{x}_i), \tag{1}$$

and $\phi(\vec{x} - \vec{x}_i)$ are peaks centered around the baryon location x_i with wave function width in configuration space $\sim\Lambda_{\rm QCD}^{-1}$, the confinement scale (Fig. 1). We approximate ϕ by Gaussian wave packets

$$\phi(\vec{x} - \vec{x}_i) = \exp[-(\vec{x} - \vec{x}_i)^2 \Lambda_{\rm QCD}^2]. \tag{2}$$

The advantage of this *Ansatz* is that the mean field in a given event can be solved analytically: The quark density in momentum space, assuming a baryon is a classical mean field of quarks, will be $\Psi^2(k)$, where

$$\tilde{\Psi}(k) \propto \sum_i \tilde{\phi}(\vec{k}, \vec{x}_i), \tag{3}$$

and where $\tilde{\phi}$ are the baryonic quark wave functions

$$\tilde{\phi}(k, x_i) \propto \exp[i\vec{k}\vec{x}_i - \vec{k}^2/\Lambda_{\rm QCD}^2]. \tag{4}$$

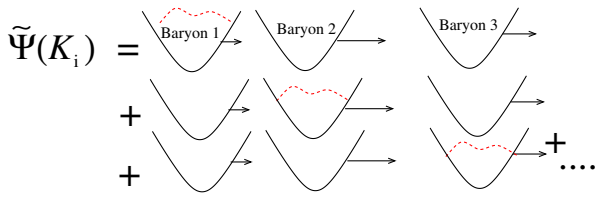

FIG. 1 (color online). Form of the quark wave function in quarkyonic matter in one dimension, as a red dashed wavy line. Baryons are represented by semiclassical black potentials wells. Arrows depict the motion of the baryons.

The space coordinates at each time step $\vec{x}_i$ are extracted from a URQMD [27,28] simulation. Note that the configuration space position of the baryon enters the wave function as a phase factor, to be multiplied with momentum. The scattering rate will therefore pick up interference terms, a crucial effect for momentum anisotropy. The important parameter in our calculation is the size of the baryon "bag" $\sim\Lambda_{\rm QCD}^{-1}$, compared to the URQMD-extracted distribution of baryons. The "bag size" is relatively insensitive to in-medium modifications, in particular to a partial restoration of chiral symmetry (see discussion in Ref. [20]). Hence, in-medium modifications of vacuum hadron-hadron cross sections used in URQMD should not impact the photon spectrum observables discussed here. We calculate Pb-Pb collisions at $\sqrt{s} = 7.7$ GeV, within the Facility for Antiproton and Ion Research (FAIR) energy range. We expect the $\sqrt{s}$ and system size dependence of them to be weak, allowing comparisons with any of Refs. [2–5].

What are the observable consequences of such dynamics? Electromagnetic signals are sensitive to the earliest, densest phase. Unlike, for example, hydrodynamic observables (that depend on the equation of state), the form factors directly influence the final spectrum. Hence, the exploration of the spectra of electromagnetic particles is an obvious place to distinguish between quarkyonic phases and more conventional quark-gluon plasma (QGP). The first observable we look at is photon production from quark-quark pQCD scattering. Photons (unlike, e.g., dileptons discussed in Ref. [20]) are not so sensitive to parameters such as the degree of thermalization of quarks and holes, about which little is known.

To understand what process is most relevant for photon production in quarkyonic matter, we have to remember that quarks are delocalized by density effects, rather than deconfinement. Hence, antiquarks and gluons remain localized [12–14,29] and can be safely neglected within baryon structure functions at this T, μ_Q. The $qg \to q\gamma$, $q\bar{q} \to g\gamma$ processes, dominating in a QGP [30,31], can be neglected, as can all processes with outgoing gluons and antiquarks. The leading quark-level production process is then quark-quark bremsstrahlung. Its scattering matrix, studied in Ref. [32], is

$$\mathcal{M}^2 = L^2(k_1, k_2 \to k_3, k_4, p) + L^2(k_1 \leftrightarrow k_2, k_3 \leftrightarrow k_4) \tag{5}$$

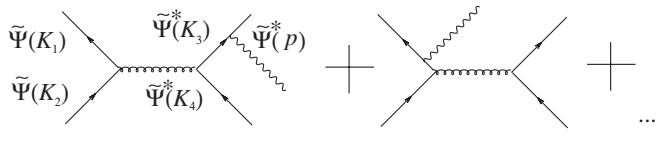

FIG. 2. pQCD process we are examining. The emitted photon is denoted by a wavy line, the spring line is a gluon, and the solid lines are quarks. The dominant process is $qq \to qq\gamma$ bremsstrahlung, which naturally leads for quarkyonic matter. Exchange diagrams can be obtained with the usual permutations.

in terms of the fine structure constant e and the QCD coupling constant λ. Here,

$$L^2 = -\frac{1}{4}e^2\lambda^2 N_c^{-2}(k_2-k_4)^{-4}\mathrm{Tr}[\not k_4\gamma^\sigma \not k_2\gamma_\rho]\mathrm{Tr}[\not k_3 Z^\mu_\sigma \not k_1 Z^\rho_\mu]$$

and $Z^\beta_\alpha = \gamma_\alpha(k_1-p)^{-1}\gamma^\beta + \gamma^\beta(k_3+p)^{-1}\gamma_\alpha$.

The photon rate convoluting the pQCD matrix and the wave function of quarkyonic matter is then

$$\frac{dN_\gamma}{d^3p} \propto \int [\mathcal{M}\tilde{\Psi}(k_1)\tilde{\Psi}^*(k_2)]^2 d^3k_{1,2,3,4} \tag{6}$$

where $\mathcal{M}$ is the matrix element corresponding to the diagrams in Fig. 2 and Eq. (5); production of a photon by the strong scattering of two quarks [32] and $\tilde{\Psi}$ is given by Eq. (3). Confinement, in both cases, is incorporated by removing quarks and gluons with momentum and virtuality $\leq \Lambda_{\mathrm{QCD}}$.

$$\int d^3k_{1,2,3,4} \to \int_{\Lambda_{\mathrm{QCD}}}^{\infty} k^2_{1,2,3,4}dk_{1,2,3,4}\int d\Omega_{1,2,3,4} \times \Theta((k_1+k_3)^2-\Lambda^2_{\mathrm{QCD}}) \times \Theta((k_2+k_4)^2-\Lambda^2_{\mathrm{QCD}}),$$

which also takes care of collinear divergences. For the quarkyonic phase, Eq. (6) is calculated for each time step in each event, with the quark wave function reflecting baryon location for that event. An average over URQMD events is then obtained. The integral in Eq. (6) was done by Monte Carlo integration, and the results, in particular the fluctuation in the last figure, were verified to be independent of statistics, both within and across events. No quark flow as separate from baryonic flow is included, as this would require separation of quarks from baryonic wave functions. Baryons, however, do develop collective flow due to the comparatively strong baryon-baryon interactions, because of both the scattering and mean field that URQMD incorporates. The backreaction of quarks to baryon flow is not understood (subleading in N_c), but the "boosted quarkyonic" scenario, described later, can be understood as an upper limit.

As a comparison, we also present the rate for an expanding thermalized quark-gluon plasma. As we do not consider the processes in Refs. [30,31] this comparison is rough, but because we are concentrating on spectra whose shapes are contained by local thermalization, the matrix element in Eq. (5) is sufficient for a qualitative estimate. The only difference between a QGP and quarkyonic matter that the incoming quark distribution functions are boosted thermal, with temperature T

$$\tilde{\Psi}(k)\tilde{\Psi}^*(k') \propto \delta(k'-k)\exp(-u_\mu k^\mu/T). \tag{7}$$

Flow u_μ includes longitudinal expansion across the kinematic range parametrized by longitudinal flow rapidity y_L and a transverse expansion $v_T(\phi) = v + v_{2T}\cos(\phi)$

$$u^\mu = \frac{1}{\sqrt{1-\tanh(y_L)^2 - v_T(\phi)^2}}\begin{pmatrix} 1 \\ v_T(\phi)\cos(\phi) \\ v_T(\phi)\sin(\phi) \\ \tanh(y_L)\end{pmatrix}. \tag{8}$$

We have checked that the results presented later, in both the quarkyonic and thermal *Ansätze*, are qualitatively similar if the QGP-appropriate $qg \to q\gamma$, $q\bar{q} \to g\gamma$ scattering processes are used in lieu of bremsstrahlung. The results shown below are determined by the form of the wave function rather than the matrix element.

We now plot the transverse momentum (p_T) distributions as well as harmonic distributions with respect to the reaction plane $\Delta\phi = \phi - \phi_{\mathrm{RP}}$. The latter is parametrized with the v_n coefficients, of which v_2 is the best-known example, as

$$\frac{dN_\gamma}{d^3p} = \frac{dN_\gamma}{dydp_T^2}\left(1 + 2\sum_{n=1}^{\infty} v_n(p_T, y)\cos(\Delta\phi)\right). \tag{9}$$

The discussion above makes it clear that quarkyonic matter and the most "normal" QGP can not, in general, coexist: quarkyonic matter defined here is not simply a "colder denser" QGP, but a state where finite density-driven delocalization, which, due to the "high" baryon mass, is nearly vertical on the T-μ_B axis on the phase diagram (see Fig. 2 of Ref. [12]). Independently of initial chemical potential, cooling curves of the system created in heavy ion collisions are also steep on the T-μ_B axis [33]. Therefore, quarkyonic matter should not appear in the cooling of a hotter QGP: quarkyonic matter and QGP should appear as alternative scenarios and should not coexist within the same event (in this sense, the constituent quark gas in Ref. [34] is *not* quarkyonic matter).

We also compare our model to calculations of direct photons from purely hadronic URQMD. For this, we employ the model developed in Ref. [35], in which hadronic scatterings from URQMD are considered as potential photon sources. The set of channels for photon production and their differential cross sections are taken from Kapusta *et al.* [31]. They include scatterings of π, ρ, and η mesons. Photons from scatterings at high momentum transfer are neglected in calculations at FAIR energies.

Missing in any $N_c \to \infty$ calculation are quark boosts due to finite baryon momentum, since baryons in this limit are static. Due to the delocalization of quarks, the consequences of finite momentum baryons are actually not so trivial, but they will always come with a N_c^{-1} factor, consistent with the hierarchy between "light" quarks and heavy baryons. In an $N_c = 3$ world, corrections to this might be significant. To estimate qualitatively the effect of these corrections, we choose a baryon at random in URQMD and "localize" the quark to that baryon, Lorentz boosting the quark by the baryon's momentum. Since baryons have some flow on average, this boosts the flow of the quarks. This distinguishes quarkyonic from boosted quarkyonic in

the plots. While this is not a quantitative estimate, it is an "extreme scenario," where a delocalized quark receives a "full boost" from one particular baryon. Hence, in a sense, it provides an upper limit as to how large the baryonic flow contribution can be without quarks becoming the actively flowing degrees of freedom.

Similarly, this model is noncausal, since the quark wave functions adjust to baryon movement instantaneously. This is another artifact of the approximation discussed above, fixed by $\sim N_c^{-1}$ contributions, but *not* improved by the localization *Ansatz*. Improving on this approximation would mean making quarks off shell, in a way that impacts baryon dynamics (or backward-in time signal propagation would occur). For longitudinal dynamics, where typical baryon longitudinal rapidity $y_L \sim 1$, this could be a significant issue, but for transverse dynamics, where baryon speeds $y_T \ll 1$, this can safely be ignored since quarks are much faster than baryons. Our most interesting results are indeed transverse. The results are shown in Fig. 3 for transverse momentum distribution and in Fig. 4 for the elliptic flow of bremsstrahlung direct photons, at impact parameter $b = 0$, 8 fm (rapidity distributions are quantitatively similar between the three models and qualitatively match experimental data). Normalization is arbitrary, as it is highly dependent on the undetermined strong coupling constant in the quark-quark scattering processes. Any determination of quarkyonic matter would come from the *shape* of the distributions.

Figure 3 shows that the p_T distribution for quarkyonic matter is distinctively steeper than realistic thermal curves or the URQMD analysis. To reproduce it with a thermal curve, an unrealistically low mean temperature has to be used, one well below deconfinement, even at realistically large chemical potential. A steep p_T distribution, therefore, can be considered as a possible signature for quarkyonic matter.

We note that this steepness is natural to explain within quarkyonic assumptions: quarks are delocalized and, hence, do not feel the flow of any particular hadron.

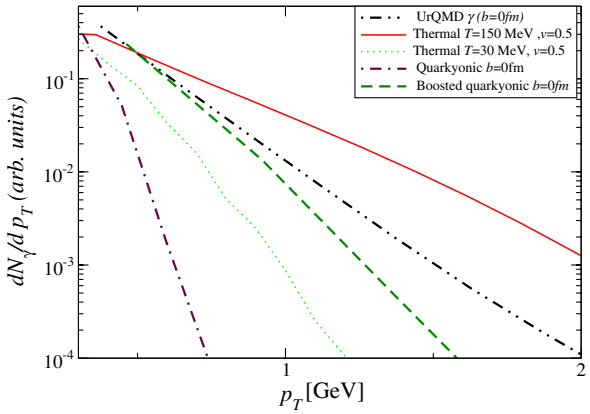

FIG. 3 (color online). Photon transverse momentum distribution for quarkyonic matter and thermalized QGP.

Boosted URQMD, unsurprisingly, is much less steep, but still well on the low side for temperature ($T \sim 30$ MeV), less than both hadronic and partonic dynamics [36–40].

While photon elliptic flow and spectra in general have yet to be measured for the energies discussed here, previous experience [41,42] suggests photon flow follows hadron flow closely. The latter, to a good approximation, is energy independent when binned with p_T [43]. While this is something hydrodynamic and transport models have yet to account properly [43,44], we can use it to extrapolate (thick line in Fig. 4).

While the flowing *Ansatz* reproduces the observed trends with the right choice of parameters, quarkyonic v_2 is something qualitatively different: Overall v_2 is compatible with zero, but with strong variations *both* event by event *and* within the same event in different p_T bins. This spread is approximately constant with centrality. This, while completely different from anything seen before, is actually physically not surprising: If baryons are not moving, the only source of v_2 is the effects of the baryon distribution on the quark wave function. The latter oscillate with a frequency $\sim p_T \rho_B^{-1/3}$ in an event-by-event dependent manner, determined by both the density and the quark momentum. The interbaryon distance $\rho_B^{-1/3}$ is highly inhomogeneous, both within the same event and event by event. Hence, both that $v_2 = 0$ overall and its random oscillation are not surprising.

For the experimental observability of this pattern, however, one must keep into account that it is generated by wave functions. Figure 4 is calculated in the limit of "many photons per event" as well as "many events," since it is in this limit that correlations due to the wave function shape become observable. The oscillation amplitude and frequency, given many photons per event, will *not* depend on the number of events, but only on $\rho_B^{-1/3}$ via the phase in Eq. (3), given by URQMD. In this limit, with p_T bins narrower than $\rho_B^{1/3}$, the photon event-by-event v_2 will

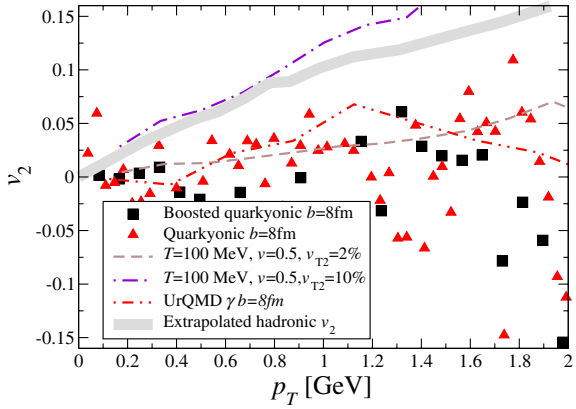

FIG. 4 (color online). Photon v_2 for quarkyonic matter and thermalized QGP. See text for an explanation of the main result, the v_2 spread, which is independent of binning and statistics. An extrapolation from hadron v_2 is also shown.

vary randomly with the amplitude and frequency given by Fig. 4. Away from this limit [$\sim O(1)$ direct photon per event], a zero v_2 at all p_T will be observed.

Since this result is unaffected by baryonic flow (boosted quarkyonic also has average zero v_2), however, the collapse of average v_2 can also be used as an indication of the quarkyonic phase, since photon v_2 is present in both QGP and hadrons (where anisotropies are dominated by flow rather than wave function shape). As the URQMD simulation in Fig. 4 shows, hadronic admixture, in particular photon decays from final-state hadrons, does not alter this conclusion because of the low $v_2(p_T)$ of direct photons in a hadronic medium.

If $>O(1)$ direct photons per event are detected and average v_2 is negligible, it is possible to look for the random fluctuations we describe, since v_2 oscillates by momentum bin and not just by event: A minimum of γ v_2 in a $\sqrt{s}$ scan, associated with an increase of v_2 fluctuations separated from reaction-plane correlated charged particle harmonics, might be a signal for the onset of a quarkyonic-dominated regime. Reference [45] discusses ways to perform such an analysis.

In conclusion, we calculated the p_T and harmonic distribution of photons from quarkyonic matter, defined as a gas of perturbative quarks moving in a baryon-generated classical potential. We found that the photon spectrum is steeper than that expected from a QGP or a hadron gas [36] at similar temperature and v_2 oscillates in a way different from both partonic and hadronic regimes. This difference can be understood from the shape of quark wave functions. Provided the quarkyonic regime dominates over QGP and the fluctuating component can be isolated, this effect can be developed into an experimental signature of quarkyonic matter.

We acknowledge the financial support received from the Helmholtz International Centre for FAIR within the framework of the LOEWE program (Landesoffensive zur Entwicklung Wissenschaftlich-Ökonomischer Exzellenz) launched by the State of Hesse. This research used resources of the Oak Ridge Leadership Computing Facility at the Oak Ridge National Laboratory, which is supported by the Office of Science of the U.S. Department of Energy under Contract No. DE-AC05-00OR22725. G. T. also acknowledges support from DOE under Grant No. DE-FG02-93ER40764. We thank the organizers of the FAIRNESS meeting, where the idea for of this work was initially developed, and Olena Linnyk and Mauricio Martinez Guerrero for discussions and suggestions.

*torrieri@fias.uni-frankfurt.de
†svogel@fias.uni-frankfurt.de
‡baeuchle@th.physik.uni-frankfurt.de

[1] K. Fukushima and C. Sasaki, arXiv:1301.6377 [Prog. Part. Nucl. Phys. (to be published)].
[2] P. Staszel (CBM Collaboration), Acta Phys. Pol. B **41**, 341 (2010).
[3] N. Antoniou *et al.* (NA49-future Collaboration), Report No. CERN-SPSC-2006-034.
[4] A. N. Sissakian and A. S. Sorin (NICA Collaboration), J. Phys. G **36**, 064069 (2009).
[5] G. Odyniec, Acta Phys. Pol. B **40**, 1237 (2009).
[6] Z. Fodor and S. D. Katz, Phys. Lett. B **534**, 87 (2002).
[7] C. R. Allton, M. Doring, S. Ejiri, S. J. Hands, O. Kaczmarek, F. Karsch, E. Laermann, and K. Redlich, Phys. Rev. D **71**, 054508 (2005).
[8] P. de Forcrand and O. Philipsen, Nucl. Phys. **B642**, 290 (2002).
[9] M. A. Stephanov, Proc. Sci., LAT 2006 (**2006**) 024.
[10] A. Casher, Phys. Lett. **83B**, 395 (1979).
[11] L. Y. Glozman, Phys. Rev. D **80**, 037701 (2009).
[12] L. McLerran and R. D. Pisarski, Nucl. Phys. **A796**, 83 (2007).
[13] T. Kojo, Y. Hidaka, K. Fukushima, L. McLerran, and R. D. Pisarski, Nucl. Phys. **A875**, 94 (2012).
[14] L. Y. Glozman, V. K. Sazonov, and R. F. Wagenbrunn, arXiv:1111.0949.
[15] S. Hands, S. Kim, and J. I. Skullerud, Phys. Rev. D **81**, 091502 (2010).
[16] A. Andronic *et al.*, Nucl. Phys. **A837**, 65 (2010).
[17] L. McLerran, K. Redlich, and C. Sasaki, Nucl. Phys. **A824**, 86 (2009).
[18] K. Miura, T. Z. Nakano, and A. Ohnishi, Prog. Theor. Phys. **122**, 1045 (2009).
[19] S. Hands, S. Kim, and J.-I. Skullerud, Phys. Rev. D **81**, 091502 (2010).
[20] S. Lottini and G. Torrieri, arXiv:1204.3272.
[21] E. Witten, Nucl. Phys. **B160**, 57 (1979).
[22] A. V. Manohar, 1997 Les Houches Lectures, arXiv:hep-ph/9802419.
[23] G. Torrieri, S. Lottini, I. Mishustin, and P. Nicolini, Acta Phys. Pol. B Proc. Suppl. **5**, 897 (2012).
[24] P. Nicolini and G. Torrieri, J. High Energy Phys. 08 (2011) 097.
[25] G. Torrieri and I. Mishustin, Phys. Rev. C **82**, 055202 (2010).
[26] S. Lottini and G. Torrieri, Phys. Rev. Lett. **107**, 152301 (2011).
[27] S. A. Bass, M. Belkacem, M. Bleicher, M. Brandstetter, L. Bravina, C. Ernst, L. Gerland, M. Hofmann *et al.*, Prog. Part. Nucl. Phys. **41**, 255 (1998).
[28] M. Bleicher, E. Zabrodin, C. Spieles, S. A. Bass, C. Ernst, S. Soff, L. Bravina, M. Belkacem *et al.*, J. Phys. G **25**, 1859 (1999).
[29] J. de Boer, B. D. Chowdhury, M. P. Heller, and J. Jankowski, Phys. Rev. D **87**, 066009 (2013).
[30] A. Dumitru, D. H. Rischke, H. Stoecker, and W. Greiner, Mod. Phys. Lett. A **08**, 1291 (1993).
[31] J. I. Kapusta, P. Lichard, and D. Seibert, Phys. Rev. D **44**, 2774 (1991); **47**, 4171(E) (1993).
[32] P. Aurenche and J. Lindfors, Nucl. Phys. **B168**, 296 (1980).
[33] J. Steinheimer, M. Bleicher, H. Petersen, S. Schramm, H. Stocker, and D. Zschiesche, Phys. Rev. C **77**, 034901 (2008).

[34] L. P. Csernai, Y. Cheng, S. Horvat, V. K. Magas, I. N. Mishustin, E. Molnar, D. Strottman, and M. Zetenyi, Proc. Sci., CPOD 2009 (**2009**) 022.
[35] B. Bäeuchle and M. Bleicher, Phys. Rev. C **81**, 044904 (2010).
[36] B. Bäeuchle and M. Bleicher, Phys. Lett. B **695**, 489 (2011).
[37] S. Turbide, R. Rapp, and C. Gale, Phys. Rev. C **69**, 014903 (2004).
[38] S. Turbide, C. Gale, and R. J. Fries, Phys. Rev. Lett. **96**, 032303 (2006).
[39] P. Huovinen, M. Belkacem, P. J. Ellis, and J. I. Kapusta, Phys. Rev. C **66**, 014903 (2002).
[40] C. Gale, S. Turbide, E. Frodermann, and U. Heinz, J. Phys. G **35**, 104119 (2008).
[41] D. Lohner (ALICE Collaboration), $\sqrt{s_{NN}} = 2.76$ TeV.
[42] A. Adare *et al.* (PHENIX Collaboration), Phys. Rev. Lett. **109**, 122302 (2012).
[43] L. Adamczyk *et al.* (STAR Collaboration), $\sqrt{s_{NN}} =$ 7.7–39 GeV, Phys. Rev. C **86**, 054908 (2012).
[44] G. Torrieri, B. Betz, and M. Gyulassy, arXiv:1208.5996.
[45] L. P. Csernai, G. Eyyubova, and V. K. Magas, Phys. Rev. C **86**, 024912 (2012).